COMMUNICATIONS IN NUMERICAL METHODS IN ENGINEERING
Commun. Numer. Meth. Engng 2008; **24**:1863–1871
Published online 19 November 2007 in Wiley InterScience (www.interscience.wiley.com). DOI: 10.1002/cnm.1073

Algorithm for analysis of periodic oscillations of structural systems with geometric nonlinearity

Minvydas Ragulskis[1,*,†] and Kazimieras Ragulskis[2]

[1] *Department of Mathematical Research in Systems, Kaunas University of Technology, Kaunas, Lithuania*
[2] *Department of Technical Sciences, Lithuanian Academy of Sciences, Vilnius, Lithuania*

SUMMARY

An algorithm for analysis of periodic oscillations of forced elastic systems with geometric nonlinearity is presented in this paper. Modal decomposition of the solution, computation of periodic oscillations for every eigenmode and estimation of geometric nonlinearities using the method of initial deformations enable to construct a computational technique that can be very effective in computation of steady-state periodic motions of slightly damped structures under periodic forcing. It is shown that the developed algorithm can be successfully exploited for the calculation of structural response of a micromechanical cantilever. Copyright © 2007 John Wiley & Sons, Ltd.

Received 3 April 2007; Revised 3 October 2007; Accepted 8 October 2007

KEY WORDS: periodic oscillation; geometric nonlinearity; finite element method

1. INTRODUCTION

Geometrical nonlinearities play an important role in the dynamics of different structures, especially when the deflections from the state of equilibrium are large [1–3]. Accurate computational representation of these nonlinearities helps to reconstruct realistic dynamical processes taking place in such systems [4–6].

Large deflections, especially large amplitude vibrations, play an important role in dynamics of micromechanical systems. A typical example is presented in [7] where a large-amplitude vibrating cantilever scanning force microscope is analysed numerically using an integrated Lennard-Jones-type attractive force in combination with a repulsive indentation force. Analysis of large amplitude vibrations of a tapered cantilever beam [8] and cantilever with a tip mass [9] helps to reveal dynamic peculiarities of those systems in resonance and forced modes of oscillation. Geometrical,

*Correspondence to: Minvydas Ragulskis, Department of Mathematical Research in Systems, Kaunas University of Technology, Kaunas, Lithuania.
†E-mail: minvydas.ragulskis@ktu.lt

material, inertial, boundary nonlinearities can be implemented into the mathematical formulations describing the dynamics of the analysed micromechanical systems. Moreover, analysis of transient dynamical processes helps to reveal complex and even chaotic behaviour of periodically forced electrostatically or parametrically actuated microcantilever systems [10–13].

The algorithm developed in this paper is based on a different concept. First of all it is assumed that external forcing is periodic but not parametric, so that the external forces depend only on time. Secondly, it is assumed that the system settles into a periodic (not necessarily harmonic) motion after the transients cease. Inherent geometric nonlinearity is taken into account using the method of initial deformations [14], and an algorithm is proposed for computation of forcing augmentation caused by geometric nonlinearity. This algorithm can be especially effective when steady-state periodic motions of undamped or slightly damped structural systems are to be calculated.

Let us consider the following matrix differential equation arising from the finite element discretization of a dynamical system:

$$[M]\{\ddot{\delta}(t)\}+[C]\{\dot{\delta}(t)\}+[K]\{\delta(t)\}=\{F(t)\} \tag{1}$$

where $[M]$ and $[K]$ are mass and stiffness matrixes (both symmetric and positive definite); $[C]=\alpha[M]+\beta[K]$; α and β are external and internal damping coefficients; $\{\delta(t)\}$ is column vector of nodal displacements; top dots denote derivatives with respect to time t and $\{F(t)\}$ is nodal external load vector. It is assumed that all nodal loads are periodic functions of time; the period of excitation is equal to P.

Modal decomposition of the solution yields

$$\{\delta(t)\}=[\{\delta_1\}\cdots\{\delta_m\}]\begin{Bmatrix} z_1(t) \\ \vdots \\ z_m(t) \end{Bmatrix}=[\Delta]\{z(t)\} \tag{2}$$

where $\{\delta_i\}$ is the ith eigenmode of the undamped system and $z_i(t)$ is the modal decomposition coefficient of the ith eigenmode; $i=1,\ldots,m$; m is the number of the first eigenmodes used for approximation. From the condition of orthogonality of the eigenmodes, it follows that

$$\begin{aligned} [\Delta]^{\mathrm{T}}[M][\Delta]&=[I] \\ [\Delta]^{\mathrm{T}}[K][\Delta]&=[\Lambda] \end{aligned} \tag{3}$$

where $[I]$ is the identity matrix; $[\Lambda]$ is a diagonal matrix of eigenfrequencies:

$$[\Lambda]=\begin{bmatrix} \omega_1^2 & \cdots & 0 \\ \vdots & \ldots & \vdots \\ 0 & \cdots & \omega_m^2 \end{bmatrix}$$

ω_i is the ith eigenfrequency; $i=1,\ldots,m$.

Substituting Equation (2) into Equation (1) and multiplying by $[\Delta]^{\mathrm{T}}$ yield

$$[I]\{\ddot{z}(t)\}+(\alpha[I]+\beta[\Lambda])\{\dot{z}(t)\}+[\Lambda]\{z(t)\}=[\Delta]^{\mathrm{T}}\{F(t)\} \tag{4}$$

This produces m separate ordinary differential equations:

$$\ddot{z}_i(t)+2\omega_i c_i \dot{z}_i(t)+\omega_i^2 z_i(t)=f_i(t), \quad i=1,\ldots,m \tag{5}$$

where $c_i=\frac{1}{2}(\alpha/\omega_i+\beta\omega_i)$; $f_i(t)=\{\delta_i\}^{\mathrm{T}}\{F(t)\}$.

2. COMPUTATION OF PERIODIC OSCILLATION FOR ONE EIGENMODE

We are interested in steady-state solution of the ith differential equation of Equation (5). In general, the analysed system can be nonlinear and can exhibit quasiperiodic, yet chaotic motions even under harmonic forcing. Nonetheless we do not consider the nonlinearities essential and assume that the steady-state solution is periodic (not necessarily harmonic); its period being the same as that of the force of excitation.

We split the period P into n equal intervals (Figure 1). Interval length is T; the starting moment of the period is t_0; terminal moment is t_0+nT and coincides with t_0 due to the periodicity of the analysed process. Four node Lagrange finite elements are used to interpolate the solution in every time interval, but only the middle third of every element (shown in grey in Figures 1 and 2) is exploited to integrate the solution.

Galerkin method [14] is exploited to minimize the residual in the jth time interval:

$$\int_{t_0+(j-1)T}^{t_0+jT}[N(t)]^{\mathrm{T}}(\ddot{z}_i(t)+2\omega_i c_i \dot{z}_i(t)+\omega_i^2 z_i(t)-f_i(t))\,\mathrm{d}t=0 \tag{6}$$

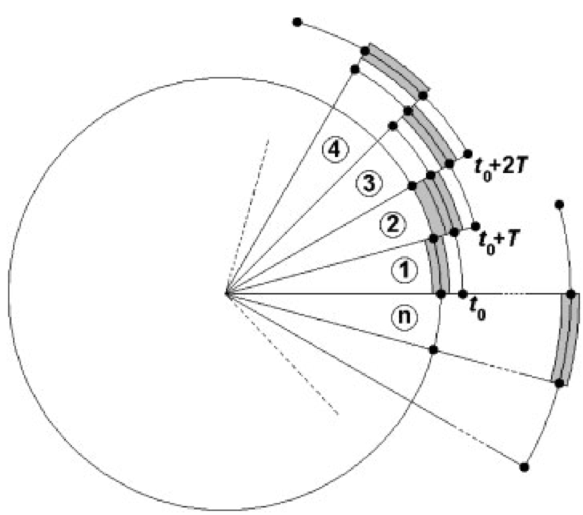

Figure 1. Meshing of the periodic solution in time.

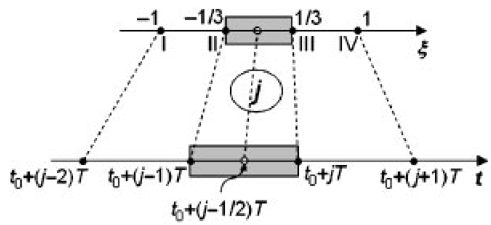

Figure 2. Transformation from local to global coordinates.

where $[N(t)]$ is a row of four consecutive shape functions of the jth finite element in time (Figure 2). Clearly, $z_i(t)$ can be approximated (in the time domain of integration) in the domain of the jth finite element:

$$z_i(t_0+(j-1)T \leqslant t \leqslant t_0+jT)=[N(t)]\{z_i^{(j)}\} \tag{7}$$

where

$$\{z_i^{(j)}\}=\begin{Bmatrix} z_i(t_0+(j-2)T) \\ z_i(t_0+(j-1)T) \\ z_i(t_0+jT) \\ z_i(t_0+(j+1)T) \end{Bmatrix}$$

If n is sufficiently large then $f_i(t)$ can be assumed constant in the middle third part of the jth finite element in time; hence, it is assumed that

$$f_i(t_0+(j-1)T \leqslant t \leqslant t_0+jT)=f_i(t_0+(j-0.5)T)=f_i^{(j)} \tag{8}$$

Integration of $\ddot{z}_i(t)$ by parts in Equation (6) and keeping Equations (7) and (8) in force yield

$$\begin{aligned} &[N(t)]^{\mathrm{T}}\dot{z}_i(t)\Big|_{t_0+(j-1)T}^{t_0+jT} \\ &\quad+\int_{t_0+(j-1)T}^{t_0+jT}(-[\dot{N}(t)]^{\mathrm{T}}[\dot{N}(t)]+2\omega_i c_i[N(t)]^{\mathrm{T}}[\dot{N}(t)]+\omega_i^2[N(t)]^{\mathrm{T}}[N(t)])\,\mathrm{d}t\{z_i^{(j)}\} \\ &\quad=f_i^{(j)}\int_{t_0+(j-1)T}^{t_0+jT}[N(t)]^{\mathrm{T}}\,\mathrm{d}t \end{aligned} \tag{9}$$

Now, direct stiffness procedure [15] is performed for all time elements $j=1,\ldots,n$ (Figure 1). The first terms in Equation (9) will be eliminated due to inverse signs in the limits of integration for adjacent finite elements. These terms will also be eliminated at the boundary of the first and the last element due to the periodicity of the process. The following algebraic system of equations is produced:

$$[A]\{z_i\}=\{B\} \tag{10}$$

DOI: 10.1002/cnm

where $\{z_i\}$ is the global vector of the modal decomposition coefficients of the ith eigenmode at the nodes of the mesh in time:

$$\{z_i\} = \begin{Bmatrix} z_i(t_0) \\ z_i(t_0+T) \\ \vdots \\ z_i(t_0+(n-1)T) \end{Bmatrix}$$
$$[A] = \frac{3T}{2}\sum_{\text{D.S.}}\int_{-1/3}^{1/3}(-[\dot{N}(\xi)]^{\mathrm{T}}[\dot{N}(\xi)]+2\omega_i c_i[N(\xi)]^{\mathrm{T}}[\dot{N}(\xi)]+\omega_i^2[N(\xi)]^{\mathrm{T}}[N(\xi)])\,\mathrm{d}\xi \tag{11}$$
$$\{B\} = \frac{3T}{2}\sum_{\text{D.S.}} f_i^{(j)}\int_{-1/3}^{1/3}[N(\xi)]^{\mathrm{T}}\,\mathrm{d}\xi$$

where notation D.S. stands for the direct stiffness procedure; ξ is the local coordinate. It can be noted that the dimension of matrix $[A]$ is $n\times n$.

Analogous procedures can be repeated for all eigenmodes that would result in the determination of all $\{z_i\}$, $i=1,\ldots,m$. Then, nodal displacements can be reconstructed at every time node:

$$\{\delta(t_0+(j-1)T)\}=[\Delta]\begin{Bmatrix} z_1(t_0+(j-1)T) \\ \vdots \\ z_m(t_0+(j-1)T) \end{Bmatrix}, \quad j=1,\ldots,n \tag{12}$$

3. ALGORITHM FOR ESTIMATION OF STRUCTURAL NONLINEARITIES

So far a linear system has been analysed. The forcing is assumed to be constant in every time step (Equation (8)). Therefore, we can approximate nodal displacements of the linear system at the central point of every time step (Figure 2):

$$\{\delta(t_0+(j-0.5)T)\}=\sum_{k=1}^{4}N_k(0)\{\delta(t_0+(j+k-3)T)\}, \quad j=1,\ldots,n \tag{13}$$

Now, geometrical nonlinearity is taken into account by the method of initial deformations [14]. We will analyse a two-dimensional nonlinear elastic structure. Geometrically nonlinear strains are evaluated through the following relationship:

$$\{\varepsilon\}=([B]+\tfrac{1}{2}[A][G])\{\delta(t)\} \tag{14}$$

where $\{\varepsilon\}$ denotes a vector of the three strain components in the domain of a finite element in space; $[B]$ is a matrix relating nodal displacements and linear strains; matrixes $[A]$ and $[G]$ account for geometric nonlinearity [14]:

$$[B]=\begin{bmatrix} \dfrac{\partial M_1(x,y)}{\partial x} & 0 & \cdots \\ 0 & \dfrac{\partial M_1(x,y)}{\partial y} & \cdots \\ \dfrac{\partial M_1(x,y)}{\partial y} & \dfrac{\partial M_1(x,y)}{\partial x} & \cdots \end{bmatrix}, \quad [G]=\begin{bmatrix} \dfrac{\partial M_1(x,y)}{\partial x} & 0 & \cdots \\ 0 & \dfrac{\partial M_1(x,y)}{\partial x} & \cdots \\ \dfrac{\partial M_1(x,y)}{\partial y} & 0 & \cdots \\ 0 & \dfrac{\partial M_1(x,y)}{\partial y} & \cdots \end{bmatrix}$$
$$\begin{Bmatrix} \dfrac{\partial u}{\partial x} \\ \dfrac{\partial v}{\partial x} \\ \dfrac{\partial u}{\partial y} \\ \dfrac{\partial v}{\partial y} \end{Bmatrix}=[G]\{\delta\}, \quad [A]=\begin{bmatrix} \dfrac{\partial u}{\partial x} & \dfrac{\partial v}{\partial x} & 0 & 0 \\ 0 & 0 & \dfrac{\partial u}{\partial y} & \dfrac{\partial v}{\partial y} \\ \dfrac{\partial u}{\partial y} & \dfrac{\partial v}{\partial y} & \dfrac{\partial u}{\partial x} & \dfrac{\partial v}{\partial x} \end{bmatrix} \tag{15}$$

where $M_l(x,y)$ are shape functions in space; l denotes current node number of the finite element in space; u and v are the displacements in the directions of x- and y-axes of the orthogonal Cartesian system of coordinates.

The principal of virtual displacements [14] yields

$$[M]\{\ddot{\delta}(t)\}+[C]\{\dot{\delta}(t)\}+\iint [B]^{\mathrm{T}}\{\sigma\}\,\mathrm{d}x\,\mathrm{d}y=\{F(t)\} \tag{16}$$

where $\{\sigma\}$ is the vector of stresses. As $\{\sigma\}=[D]\{\varepsilon\}$, where $[D]$ is the matrix of elastic constants, and keeping Equation (14) in force we produce

$$[M]\{\ddot{\delta}(t)\}+[C]\{\dot{\delta}(t)\}+\iint [B]^{\mathrm{T}}[D]\left([B]+\frac{1}{2}[A][G]\right)\mathrm{d}x\,\mathrm{d}y\{\delta(t)\}=\{F(t)\} \tag{17}$$

which leads to

$$[M]\{\ddot{\delta}(t)\}+[C]\{\dot{\delta}(t)\}+[K]\{\delta(t)\}=\{F(t)\}+\{\overline{F}(t)\} \tag{18}$$

DOI: 10.1002/cnm

where

$$\{\overline{F}(t)\} = -\frac{1}{2}\iint [B]^{\mathrm{T}}[D][A][G]\{\delta(t)\}\,\mathrm{d}x\,\mathrm{d}y \tag{19}$$

Thus, the developed iterative algorithm for analysis of geometrically nonlinear systems comprises the following basic steps:

(i) Calculate steady-state oscillations of the linear system.
(ii) Determine displacements at the central points of the time steps (Equation (13)).
(iii) Augment external load vector caused by geometric nonlinearities determined by using the methods of initial stiffness (Equation (19)).
(iv) Calculate steady-state oscillations of the system with augmented forcing (Equation (18)).
(v) Repeat from step (ii), if calculated displacements differ substantially from the previously calculated displacements. Else—stop.

4. COMPUTATIONAL EXAMPLE

A cantilever beam with motionlessly fixed left end is shown in Figure 3 (light grey mesh corresponds to the state of equilibrium). It is assumed that the middle node at the right end of the cantilever is forced by harmonic excitation in the direction of the y-axis only.

Maximum deflections of the linear system from the state of equilibrium in a period of steady-state oscillation is presented by grey mesh; maximum deflections of the nonlinear system is presented by black mesh in Figure 3. The effect of foreshortening caused by nonlinearity and observed for undamped normal modes of cantilever [16] can be clearly seen in Figure 3 where the oscillations are forced; the dynamical system is undamped; 15 first eigenmodes are taken into account for modal decomposition and five iterations are used for solution to converge.

In order to represent the dynamical process during the whole period of oscillation, we plot the trajectories of the forced node of the cantilever in the x–y plane for linear and geometrically nonlinear systems (Figure 4). Clearly, the trajectory of the node corresponding to the nonlinear system represents realistic physical scenario. It shows that the assumption of geometric nonlinearity can be an absolute necessity for numerical models in micromechanical applications. Even small differences in micro-cantilever tip deflection in macro-scale can result in enormous differences in distances in the nano-scale.

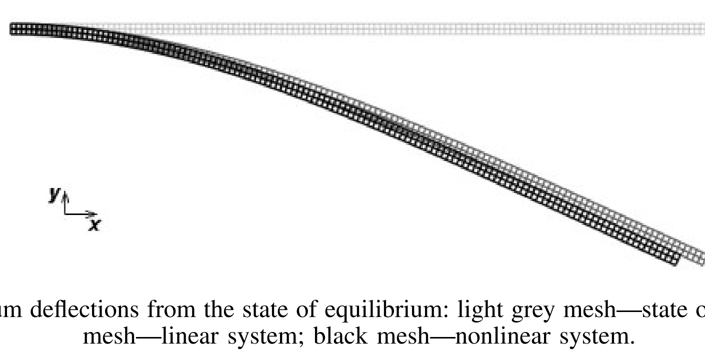

Figure 3. Maximum deflections from the state of equilibrium: light grey mesh—state of equilibrium; grey mesh—linear system; black mesh—nonlinear system.

DOI: 10.1002/cnm

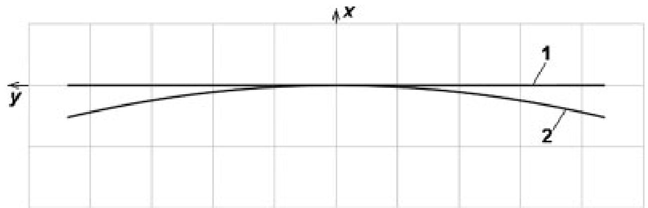

Figure 4. Trajectories of oscillation of the driven node: 1—linear system; 2—nonlinear system.

5. CONCLUSIONS

The computational technique developed for the analysis of forced periodic oscillations of geometrically nonlinear systems is applicable for a wide class of problems and can be generalized for 3D geometry. It is especially effective when geometrically nonlinear systems experience periodic forcing, are undamped or are slightly damped.

The presented algorithm for analysis of periodic oscillations of forced elastic systems with geometric nonlinearity is an iterative algorithm. The steps (iii) (augmentation of the external load vector) and (iv) (computation of displacements at augmented forcing) are to be iterated for several times till acceptable convergence is achieved. Detailed analysis of the necessary conditions and speed of convergence is a definite object of future research.

The presented method can be considered as an alternative to the Fourier decomposition techniques. Of course, Fourier decomposition or harmonic balance techniques have a definite advantage when only one or few harmonics are to be taken into account [17]. However, these advantages disappear when a large number of harmonics have to be considered and then the proposed method becomes much more effective.

REFERENCES

1. Anabili M. Theory sand experiments for large-amplitude vibrations of circular cylindrical panels with geometric imperfections. *Journal of Sound and Vibration* 2006; **298**:43–72.
2. Ye J. An alternative approach for large deflection analysis of axisymmetric plates on elastic foundation. *Communications in Numerical Methods in Engineering* 1994; **10**:623–632.
3. Miller K, Joldes G, Lance D, Wittek A. Total Lagrangian explicit dynamics finite element algorithm for computing soft tissue deformation. *Communications in Numerical Methods in Engineering* 2007; **23**:121–134.
4. Arciniega RA, Reddy JN. Tensor-based finite element formulation for geometrically nonlinear analysis of shell structures. *Computer Methods in Applied Mechanics and Engineering* 2007; **196**:1048–1073.
5. Lacarbonara W, Yabuno H. Refined models of elastic beams undergoing large in-plane motions: theory and experiment. *International Journal of Solids and Structures* 2006; **43**:5066–5084.
6. Bornemann PB, Galvanetto U. Discrete dynamics of implicit time integration schemes for a dissipative system. *Communications in Numerical Methods in Engineering* 2003; **19**:737–748.
7. Chen J, Workman RK, Sarid D, Hoper R. Numerical simulations of a scanning force microscope with a large-amplitude vibrating cantilever. *Nanotechnology* 1994; **5**:199–204.
8. Nageswara RB, Venkateswara RG. Large amplitude vibrations of a tapered cantilever beam. *Journal of Sound and Vibration* 1998; **127**:173–178.
9. Cheng G, Mei C, Lee RY. Large amplitude vibration of a cantilever beam with tip mass under random base excitation. *Advances in Structural Engineering* 2001; **4**:203–210.
10. Liu S, Davidson A, Lin Q. Simulating nonlinear dynamics and chaos in a MEMS cantilever using Poincare mapping. *Twelfth International Conference on Transducers*, *Solid-State Sensors*, *Actuators and Microsystems*, vol. 2, Boston, U.S.A., 8–12 June, 2003; 1092–1095.

DOI: 10.1002/cnm

11. Jamitzky F, Stark M, Bunk W, Heckl WM, Stark RW. Nonlinear dynamics of a microcantilever in close proximity to a surface. *Fourth IEEE Conference on Nanotechnology*, vol. 1, Munich, Germany, 16–19 August, 2004; 38–40.
12. Arafat HN, Nayfeh AH, Chin CM. Nonlinear nonplanar dynamics of parametrically excited cantilever beams. *Nonlinear Dynamics* 1998; **15**:31–61.
13. Yldrm V. Out-of-plane bending and torsional resonance frequencies and mode shapes of symmetric cross-ply laminated beams including shear deformation and rotary inertia effects. *Communications in Numerical Methods in Engineering* 2000; **16**:67–74.
14. Zienkiewicz OC, Taylor RL. *Finite Element Method—Solid and Fluid Mechanics*: *Dynamics and Nonlinearity*, vol. 2. McGraw-Hill: New York, 1991; 790.
15. Bathe KJ. *Finite Element Procedures in Engineering Analysis*. Prentice-Hall: Englewood Cliffs, NJ, 1982; 735.
16. Hsieh SR, Shaw SW, Pierce C. Normal modes large amplitude vibration of a cantilever beam. *International Journal of Solids and Structures* 1994; **31**:1981–2014.
17. Ragulskis M, Fedaravicius A, Ragulskis K. Numerical procedure for fluid flow in a pipe performing transverse oscillations. *Communications in Numerical Methods in Engineering* 2006; **22**:347–356.

DOI: 10.1002/cnm